ELSEVIER

Thermochimica Acta 273 (1996) 257–268

thermochimica acta

Thermochemical adsorptive and catalytic events occurring during isopropanol decomposition over MnO_x-modified aluminas. *In situ* infrared spectroscopic studies

M.I. Zaki[a,*], G.A.M. Hussein[b], A.K.H. Nohman[b], Y.E. Nashed[b]

[a] *Chemistry Department, Faculty of Science, Kuwait University, P.O. Box 5969, Safat 13060, Kuwait*
[b] *Chemistry Department, Faculty of Science, Minia University, El-Minia 61519, Egypt*

Received 17 March 1995; accepted 10 June 1995

Abstract

Adsorptive and catalytic events occurring at gas/solid interfaces established during isopropanol decomposition over pure and MnO_x-modified aluminas were monitored and characterized by in situ infrared spectroscopic measurements. On pure alumina the alcohol adsorbs dissociatively and non-dissociatively at room temperature, giving rise respectively to isopropoxides coordinated to Lewis acid sites and isopropanol molecules hydrogen-bonded to hydroxyl (and oxide) sites. Those adsorbed species withstand outgassing at room temperature, but are completely eliminated near 200°C. Meanwhile, the alcohol catalytic dehydration is commenced at 150°C and gas-phase propene is thus released. Quantitative conversion into the alkene is effected near 225°C. The modification with MnO_x stabilizes the isopropoxide species to thermo evacuation at well above 200°C, but activates their conversion into surface carboxylates at > 300°C. Moreover, the isopropanol dehydration selectivity of alumina is critically suppressed and acetone becomes the dominant gas-phase product. Thus, a strong dehydrogenation selectivity is generated. These and other MnO_x-influenced alterations to the adsorptive and catalytic behaviours of alumina are discussed on the basis of available characterization results for the catalysts and mechanistic aspects established in the field.

Keywords: Alumina catalysts; Infrared spectroscopy; Isopropanol catalytic decomposition; Manganese oxide-modified alumina catalysts

* Corresponding author.

SSDI 0040-6031(94)02580-4

1. Introduction

Pure transitional aluminas, particularly the γ-structured, are potential acid–base catalysts [1]. In alcohol decomposition reactions, alumina surfaces selectively catalyse the dehydration pathway [2]. Thus, isopropanol decomposition on alumina produces predominantly gas-phase propene [3]. The dehydrogenation pathway and, hence, the production of acetone are observed when the alumina is pre-outgassed under extreme conditions [4]. Under those conditions, anionic defects are increasingly generated and adjacent Al^{3+} consequently develop into notably stronger-than-normal Lewis acid sites (designated x-sites [4]). It is these sites which are believed to generate the dehydrogenation activity [4]. Alumina surfaces have been found incapable of activating either the propene or acetone thus produced for further reactions, even under conditions of slow removal of reaction products [3]. In contrast, a number of other oxides tend to involve acetone in bi-molecular surface reactions leading to secondary products, e.g. group IVB metal oxides [5] and CeO_2 [6].

The outgassing conditions necessary for the generation on alumina of active (x-) sites, include a prolonged exposure to high vacuum ($\sim 10^{-7}$ Torr) at high temperatures ($\geqslant 800°C$) [4, 7]. These conditions are impractical for applications at industrial level, and impose, moreover, catalytically unfavourable surface and bulk structural consequences. For instance, effective mass transfer is enhanced at high temperatures and the surface accessibility is thereby constricted. Therefore, chemical means operable under mild thermal conditions are employed to modify the selectivity of catalysts [8]. Additives derived from readily decomposable parent compounds, such as CrO_x from $Cr(NO_3)_3 \cdot 9H_2O$ [3], were found to develop a considerable isopropanol dehydrogenation activity on alumina. However, the accessible structure [9] and solid-state reactivity [10] of transitional aluminas enhance incursion of the modifying species into the material bulk. Catalytically unfavourable consequences may also occur [11].

In the present investigation, γ-alumina was chemically modified by addition of MnO_x using two different techniques (impregnation and coprecipitation) and subsequent calcination at moderate-to-high temperatures. MnO_x-based catalysts are known for their potential redox activity and selectivity [12, 13]. Adsorptive and catalytic consequences have been assessed versus the behaviour of pure alumina towards isopropanol vapour using in situ IR spectroscopic measurements. Such measurements have proven quite informative in analogous studies on alumina [3] and other metal oxides [5, 6]. The results are discussed in the light of (a) available characterization results monitoring bulk and surface consequences of alumina modification with MnO_x (Table 2 below), and (b) mechanistic aspects established in the field of alcohol catalysis on metal oxides [13].

2. Experimental

2.1. The aluminas

Pure alumina (denoted A) was Degussa Aluminiumoxide C (Germany). MnO_x-modified aluminas (at 10 wt% Mn) were prepared in two different ways. In the first,

pure A was impregnated with aqueous solution of Sigma $Mn(NO_3)_2 \cdot 4H_2O$ [14]. In the second, the modification was carried out via coprecipitation by addition of ammonia solution to a mixture of aqueous solutions of manganese and aluminium nitrates (ALEC/Egypt $Al(NO_3)_3 \cdot 9H_2O$) to pH ~ 9 [14]. The resulting materials (denoted MnA and MnAC, respectively) were washed till nitrate-free, dried at 10^{-2} Torr and 50°C to constant weight, and then calcined at 600 and 1000°C for 5 h. The calcination products are indicated below by a numeral symbolizing the calcination temperature applied. Thus, MnA6 is 600°C calcination product of the impregnated alumina, whereas MnAC10 is the calcination product of coprecipitated alumina at 1000°C. For control purposes, pure alumina was similarly treated in aqueous medium, dried, calcined and indicated by A6 and A10.

2.2. *Differential thermal analysis*

DTA curves were obtained for the parent, i.e. uncalcined, aluminas on heating (at $10°C\,min^{-1}$) up to 1100°C in a static air atmosphere, using a model 30H Shimadzu analyser (Japan); 15–20 mg portions of test samples were used, and α-Al_2O_3 was the thermally inert reference material (Shimadzu Corp.).

2.3. *In situ infrared spectroscopy*

In situ IR spectroscopy was carried out using self-supporting wafers of test aluminas mounted inside specially designed quartz glass IR cells and a model 580B Perkin-Elmer ratio-recording spectrophotometer (UK). The technique and procedure adopted are detailed elsewhere [5, 14]. The cells were equipped with KBr windows and the spectrophotometer with a model 3500 Perkin-Elmer data station for spectra acquisition and subtraction. The data station also facilitated quantitative assessments of gas-phase spectra (see below), implementing Perkin-Elmer QUANT software and the method described previously [5, 14].

The test wafers of alumina were pretreated in situ by heating at 500°C for 1 h in an atmosphere of oxygen flowing at 50 ml min^{-1}, cooling in oxygen, and outgassing at RT. A background spectrum was taken from the wafer, prior to exposure to 10 Torr of air-free isopropanol vapour (BDH/UK) at RT. IR spectra were then taken at room (actually beam) temperature from the "water + adsorbed species", following a 5-min outgassing period at different temperatures in the range RT-400°C. Spectra of the adsorbed species were obtained by absorption subtraction of the wafer background spectrum, by means of the on-line data station.

In another set of experiments, the wafer was heated for 10 min at different temperatures (100–400°C) in the alcohol atmosphere, and spectra were taken correspondingly from the equilibrated gas phase. A fresh (10 Torr) dose of the alcohol vapour was admitted at RT, before heating to each desired temperature. Absorptions displayed in the spectra were assigned on the basis of literature data [5, 15] and authentic spectra taken under identical spectroscopic conditions from Specpure samples of acetone, propene, isobutene, CH_4 and CO_2. The authentic materials also facilitated construct-

ing the calibration curves (absorbance vs. pressure) demanded by the computer-oriented quantitative analysis of the gas-phase spectra [5, 14].

3. Results and discussion

3.1. Calcination course of aluminas

The DTA curves exhibited in Fig. 1 show that the unmodified alumina (A) experienced the usual stepwise dehydroxylation [16,] monitored here by the three endotherms at 80–220°C, and bulk ordering into the γ-structure [9, 16] as marked by the broad exotherm near 400 °C. No other thermal events are displayed on further heating up to 1000°C. These results suggest that the calcination of alumina at 600°C and 1000°C supports the development and maintenance of the γ-structure, but reduces the amount of surface hydroxylation [17].

The modified aluminas, MnA and MnAC, are shown (Fig. 1) to exhibit DTA curves displaying similarly a broad endotherm at < 100°C, a strong exotherm at 210°C, and ill-defined endothermal behaviour at 225–300°C. Distinctively, however, MnAC exhibits a strong endotherm at 280°C, whereas MnA gives rise to a broad endotherm near 950°C. Thus the thermal behaviours of the modified aluminas are rather similar amongst themselves, but are markedly different from the behaviour of the unmodified alumina (A). Fig. 1 shows, moreover, that the similar behaviours of Mn and MnAC at

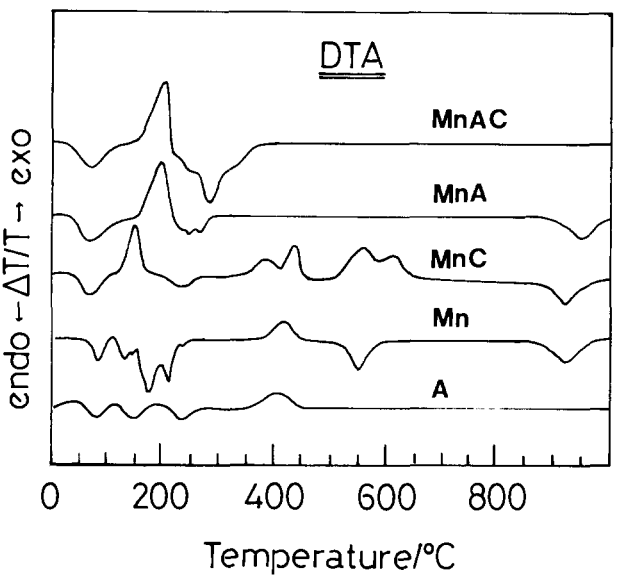

Fig. 1. Differential thermal analysis curves obtained on heating (at 10°C min^{-1}) the parent materials in static air: A, pure alumina; Mn, $Mn(NO_3)_2 \cdot 4H_2O$; MnC, α-/β-Mn_3O_4; MnA, impregnated alumina; MnAC, coprecipitated alumina.

$\leqslant 300°C$ are close to the behaviour of MnC ($= \alpha$-/β-Mn_3O_4, see Table 1), but remotely different from that of Mn ($= Mn(NO_3)_2 \cdot 4H_2O$).

According to literature data [18] reviewed in Table 1, one may consider the thermal events observed at $\leqslant 300°C$ for the modified aluminas to account for oxidation of initial Mn(II) to Mn(IV) species. This can be corroborated by the fact that MnC assumes Mn_3O_4 composition (Mn^{II}, Mn^{III}) at RT, which is transformed into Mn_5O_8 (Mn^{II}, Mn^{IV}) at higher temperatures. Other supportive results can be found in the literature [11, 19–22]. The thermal behaviours at > 300–$1000°C$ suggest that the Mn(IV) species are stabilized in the coprecipitated alumina (MnAC) better than in the impregnated one (MnA). This is corroborated by the 950°C endotherm marking the decomposition of Mn(IV) species of MnA into the low-oxidation species of Mn_3O_4 (Table 1). The closer contact between MnO_x and AlO_x species in coprecipitated MnAC may facilitate stronger solid/solid interactions between them at high temperatures, and this might be responsible for the distinct endotherm displayed at 280°C in the DTA curve of MnAC (Fig. 1).

Thus, the DTA results may account for oxidation of the primary Mn(II) species during the calcination of MnA and MnAC at 600 and 1000°C, most probably to the tetravalent state. It is a common practice of Mn(II) species to oxidize to Mn(IV) species when heated in an oxidizing environment (air, NO_3^-) [18], but it is also common that Mn(IV) species decompose at high temperatures (Table 1) into low-valent species (Mn_2O_3 and Mn_3O_4). Mn(IV) species are, however, thermally stabilized in contact with γ- and α-alumina, being accommodated in their octahedral holes [19, 20]. They are even chemically stabilized to hydrogen reduction, as has been shown by TPR

Table 1
Compositional consequences of high temperature treatments of parent materials of MnO_x, as characterized previously, see Ref. [18]

Mn ($Mn(NO_3)_2 \cdot 4H_2O$)

$$\xrightarrow{(110\text{–}210°C)} \underset{(Pyr;\ j)}{\beta - MnO_2} + \underset{(Bix;\ m)}{\alpha - Mn_2O_3} \xrightarrow{(550\text{–}600°C)} \underset{(Bix;\ s)}{\alpha - Mn_2O_3}$$

$$\xrightarrow{(900\text{–}950°C)} \underset{(Tet;\ j)}{\beta - Mn_3O_4} + \underset{(Cub;\ m)}{\gamma - Mn_3O_4}$$

MnC ($\alpha - /\beta - Mn_3O_4$)

$$\xrightarrow{(150\text{–}450°C)} \underset{(Tet;\ j)}{\alpha - /\beta - Mn_3O_4} + \underset{(Mng;\ m)}{Mn_5O_8} \xrightarrow{(550\text{–}600°C)} \underset{(Bix;\ j)}{\alpha - Mn_2O_3} + \underset{(Tet;\ m)}{\alpha - /\beta - Mn_3O_4}$$

$$\xrightarrow{(950\text{–}1000°C)} \underset{(Tet;\ j)}{\alpha - /\beta - Mn_3O_4} + \underset{(Cub;\ m)}{\gamma - Mn_3O_4}$$

Key: Pyr, pyrolusite; Bix, bixbyite; Mng, manganoxide; Tet, tetragonally distorted spinel; Cub, cubic spinel; *j*, major; *m*, minor; *s*, sole detectable.

experiments reported by Baltanas et al. [22]. This has been attributed [22] to the electronically "hard" nature of AlO_x species [23,24]. Accordingly, the relatively close contact between MnO_x/AlO_x species facilitated in the coprecipitated MnAC may help a notable stabilization of high-valent MnO_x species.

3.2. Characteristics of calcined aluminas

The calcination products of pure and modified aluminas at 600 and 1000°C were the subject of a recent, extensive investigation [25] aiming at assessing changes induced by the MnO_x modifier to the surface and bulk properties of alumina. The important results are summarized in Table 2. It is obvious that the MnO_x additives do not form detectable, separate bulk phases in any of the calcination products examined. Thus,

Table 2
Summary of important results of previous bulk and surface characterization studies of the aluminas, see, Ref. [25]

Alumina	Crystalline bulk[a]		Surface acid–base[b]		Surface area[c]
	Phase composition [d]	Structure	Behaviour[e]	Sites[d]	$/\pm 2\,m^2\,g^{-1}$
A6	γ-Al_2O_3	Spinel-like: defect structured	Moderately acidic	L-Al (*m*) $OH^{\delta+}$ (*j*) $OH^{\delta-}$ (*m*)	102
A10	γ-Al_2O_3		Moderately acidic	L-Al (*j*) $OH^{\delta+}$ (*m*) $OH^{\delta-}$ (*m*)	90
MnA6	γ-Al_2O_3		Moderately acidic–basic	L-MnAl (*j*) $OH^{\delta+}$ (*m*) $OH^{\delta-}$ (*j*)	92
MnA10	α-Al_2O_3	Corundum-like: hexagonal close packing	Strongly acidic–basic	L-MnAl (*j*) $OH^{\delta+}$ (*m*) $OH^{\delta-}$ (*j*) O^{X-} (*m*)	41
MnAC6	γ-Al_2O_3		Moderately acidic–strongly basic	L-MnAl (*m*) $OH^{\delta+}$ (*m*) $OH^{\delta-}$ (*j*) O^{X-} (*m*)	164
MnAC10	α-Al_2O_3 (*d*) and MnO_x (ill-defined)		Largely basic	L-MnAl (*m*) $OH^{\delta+}$ (*m*) $OH^{\delta-}$ (*j*) O^{x-} (*j*)	10

[a] Analysed by X-ray powder diffractometry and IR spectroscopy.
[b] Probed by pyridine adsorption and in situ IR spectroscopy.
[c] Determined by BET analysis of low-temperature nitrogen adsorption data.
[d] Relative abundance: *d*, dominant; *j*, major; *m*, minor; and *t*, trace.
[e] Lewis acidity/basicity approximated from IR absorption intensities monitored in spectra taken from adsorbed pyridine over both the ν(OH) and ν(CCN) frequency regions. No Bronsted acidity was detectable on any of the surfaces examined.

MnO_x is highly dispersed in monolayer structures and/or organized in non-crystalline bulk structures. The presence of MnO_x does not affect the bulk (γ) structure of alumina at 600°C, but it enhances its conversion into the α-structure at 1000°C. A similar observation was made by others [26, 27] and attributed [27] to formation of spinel-structured Mn_3O_4 thus facilitating the atom displacement needed to convert spinel-structured γ-Al_2O_3 into corundum-structured α-Al_2O_3. Table 1 underlines the likelihood of formation of Mn_3O_4 in the calcination course of modified aluminas.

Table 2 shows, moreover, that MnO_x does not directly affect the high accessibility of alumina surface ($102\,m^2\,g^{-1}$). It is rather the MnO_x-induced $\gamma \rightarrow \alpha$ bulk modification at 1000°C that decreases markedly the surface area (down to $10\,m^2\,g^{-1}$). However, the presence of MnO_x is shown to improve the surface Lewis acidity of alumina by influencing the primary Lewis sites (L – Al → L – MnAl) and/or generating new Lewis sites based solely on MnO_x species. It also substantiates the surface Lewis basic sites ($OH^{\delta-}$ and O^{x-}) which coexist with the acidic $OH^{\delta+}$ groups (hydrogen bond donors) exposed primarily on alumina. These results could be expected from IR carbonyl spectra taken from CO/Mn_3O_4 by Angevaare et al. [28]. The spectra have revealed the exposure on the oxide of two types of Lewis acid sites (three-fold coordinated Mn^{2+} and four-fold coordinated Mn^{3+}) and isolated OH-groups of a rather basic character.

3.3. *Isopropanol adsorptive events*

Fig. 2 compares IR spectra exhibited by adsorbed isopropanol species, established on the 600°C calcination products of pure (A6) and modified (MnA6 and MnAC6) aluminas, following outgassing at different temperatures. Quite similar spectra were exhibited by the alcohol species on the corresponding 1000°C calcination products. Therefore, the spectra demonstrated in Fig. 2 are considered as being typical, regardless of the catalyst calcination temperature.

Fig. 2 shows that irreversible adsorption of the alcohol on pure alumina (A) at RT results in low-frequency shifts of the ν(OH) vibrations of some of the isolated Al–OH groups [29] monitored in the background (Bkg) spectrum at 3800–3600 cm^{-1}. This indicates formation of hydrogen-bonded alcohol molecules (to surface $OH^{\delta+}$ and O^{2-}) [5, 6]. It is also shown that the alcohol is dissociatively adsorbed and two types of isopropoxide species are formed: (a) terminal, namely $(CH_3)_2CHO^- \rightarrow Al^{3+}$, with ν(C–O) at 1170 cm^{-1} [5]; and (b) bridging, namely $(CH_3)_2CHO^- \rightarrow (Al^{3+})_2$, with ν(C–O) at 1130 cm^{-1} [30]. Relevant absorptions are shown in the ν(CH) (2900–2700 cm^{-1}) and ν(CC) (1500–1300 cm^{-1}) frequency regions. The hydrogen-bonded alcohol molecules are shown (Fig. 2) to be partially eliminated on outgassing at 100°C. They are evacuated almost completely, together with the alkoxide species, near 200°C.

The above results indicate the occurrence of two adsorptive events at the alcohol/A interfaces at RT–100°C: (a) non-dissociative adsorption through hydrogen-bonding of the alcohol molecules to acidic Al–OH groups, and (b) dissociative adsorption resulting in isopropoxide species coordinated to surface Lewis acid sites (cus Al^{3+}). According to previous studies [5, 6], the latter event may be approximated by the

equation

$$(CH_3)_2CHOH(g) + L^{n+}(s) + O^{2-}(s) \rightarrow (CH_3)_2CHO^- \rightarrow L^{n+}(s) + OH^-(s) \quad (1)$$

for terminal alkoxides, g denotes gas and s is for surface.

The presence of MnO_x species both in the impregnated (MnA) and coprecipitated (MnAC) aluminas, is shown (Fig. 2) to enhance the stability of the isopropoxide species

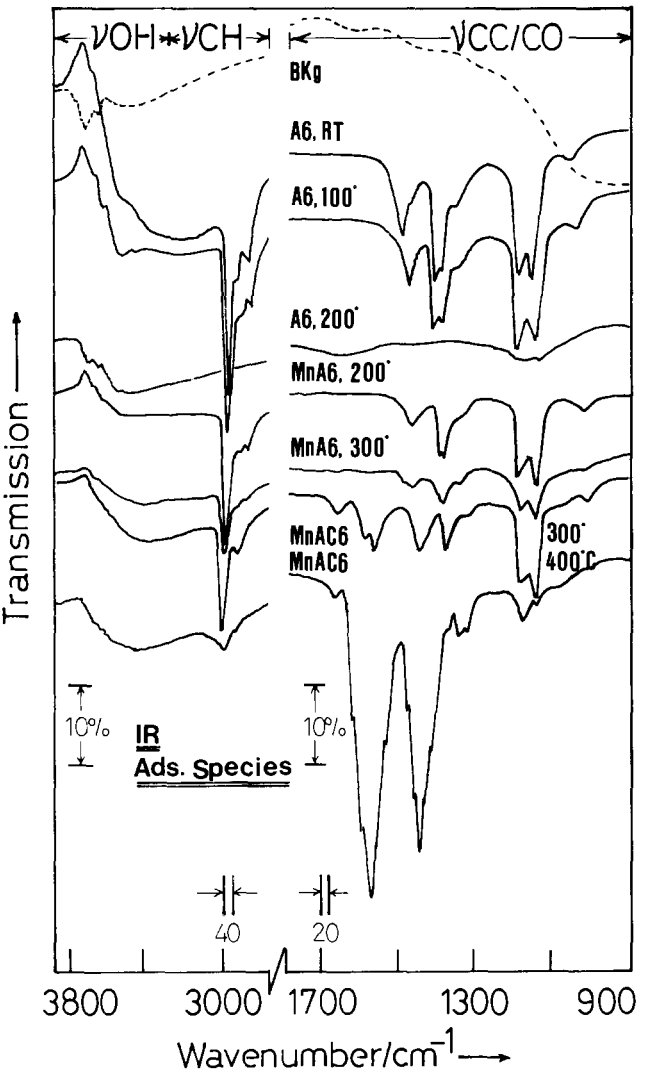

Fig. 2. In situ IR spectra of isopropanol-adsorbed species on the catalysts following exposure to the alcohol vapour (10 Torr) at RT and subsequent outgassing (for 5 min) at the temperatures indicated. BKg denotes the background spectrum taken from A6 subsequent to in situ pretreatments and prior to exposure to the alcohol atmosphere.

to high-temperature outgassing. This is most likely the effect of the MnO_x-developed Lewis acidity of alumina (Table 2). In the mean time, the stabilized isopropoxides are oxidatively converted at 300–400°C into carboxylate species (strong absorptions at 1580 and 1440 cm^{-1} [5,6]) and minority carbonate/bicarbonate species (weak twin absorptions at 1340 and 1310 cm^{-1} [31]). The weak, but distinct, absorption at 1690 cm^{-1} may, according to Fink [32], be assigned to ketonic species coordinated to the surface. The chemical modification of surface isopropoxides was also observed in a spectrum taken from isopropanol/MnA10 at 400°C (not shown), but was far more evident in a similar 400°C spectrum taken from isopropanol/MnAC10 (Fig. 2). Under similar conditions, those particular modified aluminas were found to activate coordinated pyridine for a nucleophilic attack by adjacent Lewis basic sites [25]. Surface carboxylates were also the eventual conversion products of the pyridine. According to Knözinger [33], oxidative conversion of such adsorbed species is facilitated through a concerted mechanism involving strong acid–base site-pairs. Accordingly, the interaction may be depicted by the equation

$$(CH_3)_2CHO^- \rightarrow L^{n+}(s) + OH^-(s) \rightarrow CH_3COO^- \rightarrow L^{n+}(s) + OH^-(s) + CH_4(g) \quad (2)$$

The detection of a minute amount of gas-phase CH_4 at 400°C (see below) may support Eq. (2). However, methane could equally be produced on extending the nucleophilic attack to the carboxylate species themselves; the reaction also leads to formation of surface carbonate/bicarbonate species and/or CO_2 in the gas phase. Indeed, small amounts of CO_2 are released into the gas phase at 400°C (Fig. 3 below).

The above results correlate very well with the MnO_x-influenced modifications to the acid–base behaviour of alumina surfaces (Table 2). They reflect implications of the developed Lewis acidity and basicity on the surface reactivity. Catalytic implications are discussed below.

3.4. *Isopropanol catalytic events*

Fig. 3 confirms that the alcohol decomposes almost completely at $\geqslant$ 200°C on A6, giving rise solely to gas-phase propene. A largely similar behaviour was observed on A10, as is indicated by the quantitative results demonstrated in Fig. 4A. Fig. 4A also indicates that propene thus produced remains largely unchanged on contact with the catalysts at up to 400°C. These results are in line with earlier findings regarding the dehydration selectivity of pure alumina in alcohol decomposition reactions [3,13].

Fig. 3 indicates, moreover, that the presence of MnO_x species tilts the catalytic selectivity of alumina gradually towards the dehydrogenation pathway, as evidenced by the detection of acetone in the gas phase (see also Fig. 4B and C). In apparent contrast to the sole isopropanol dehydration selectivity of pure alumina (Fig. 4A), MnAC10 exhibits sole dehydrogenation selectivity (Fig. 4C). The acetone thus produced is gradually used up at 300–400°C, due to its involvement in bi-molecular surface reactions with adsorbed molecules to produce the isobutene and methane simultaneously detected in the gas phase (Fig. 3). This is shown (Fig. 4) to occur more evidently

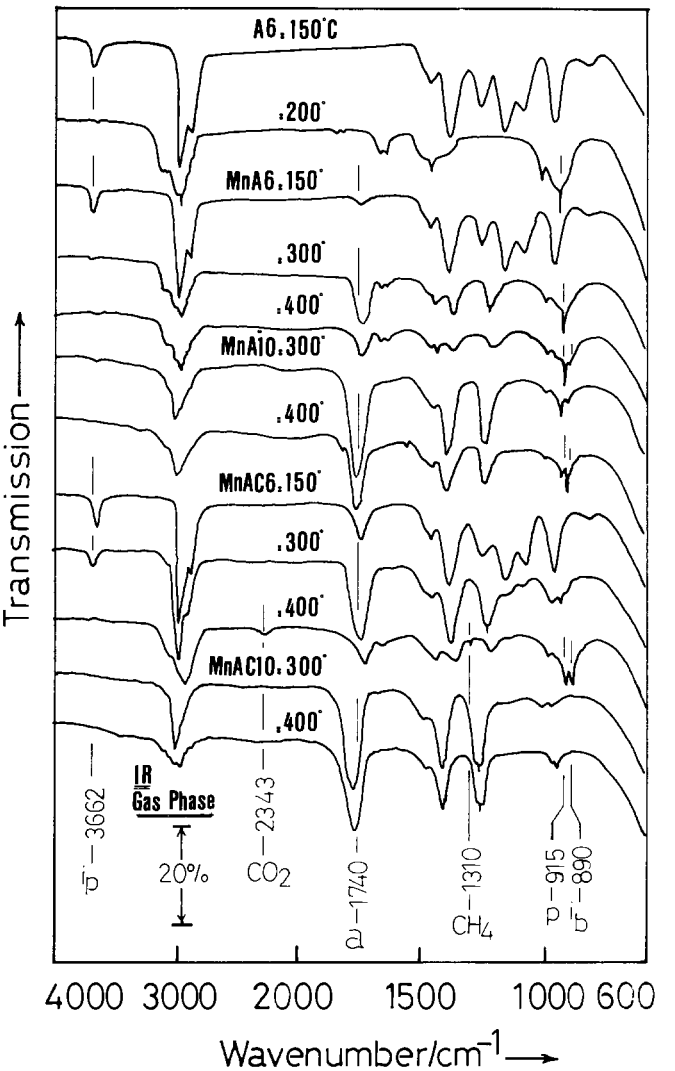

Fig. 3. In situ IR spectra of isopropanol gas phase (10 Torr) following 5-min contact intervals with the designated catalysts at the temperatures indicated. The frequencies indicated are those diagnostic to the alcohol (^{i}p) and the decomposition products: propene (p), acetone (a), isobutene (^{i}b), CO_2 and CH_4.

on the 600°C calcination products of MnA and MnAC than on the 1000°C calcination products. Previous investigations [5, 6] confirmed the surface reactions of acetone on metal oxides, and have proposed a bimolecular aldol condensation-like mechanism

$$(CH_3)_2CO(g) + (CH_3)_2CO \rightarrow L^{n+}(s) + OH^-(s) + O^{2-}(s) \rightarrow CH_3COO^- \rightarrow L^{n+}(s) + (CH_3)_2C{=}CH_2(g) + 2OH^-(s) \quad (3)$$

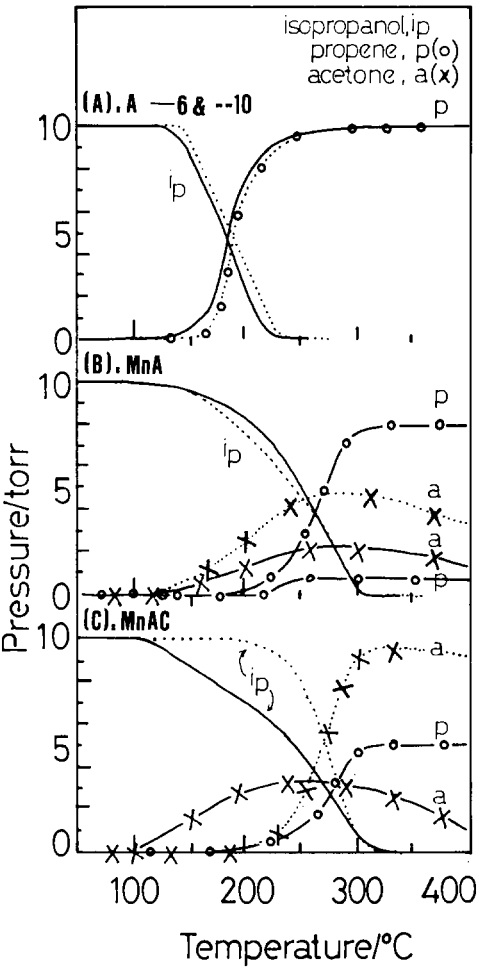

Fig. 4. IR quantitative analysis of the gas phase showing the relation between the reaction temperature and the pressure (Torr), resulting from an initial dose of 10 Torr of the reactant alcohol (^{i}p) giving rise to the primary products acetone (a; ×) and propene (p; ○) after consecutive 10-min intervals at the temperatures indicated over the catalysts calcined at 600°C (– – –) and 1000°C (···).

Eq. (3) suggests that the surface sites involved (strong acid–base site-pairs) are similar to those involved in the oxidative conversion of adsorbed isopropoxides. The moderate conduct of those sites on MnA10 and MnAC10 may be due to the bulk transformation into the closely packed α-structure and the consequent loss of surface area (Table 2).

In conclusion, the modification of γ-alumina with MnO_x (highly dispersed Mn^{IV}) species results in: (a) obvious improvement of the dissociative adsorption of isopropanol and the stability of the resulting isopropoxide surface species, (b) generation of surface oxidative reactivity towards the isopropoxide species, (c) rendering the alumina

alcohol dehydrogenation selective, and (d) activation of the surface reactivity towards acetone adsorption and further reactions. These adsorptive and catalytic consequences of the MnO_x-modification are intimately related to the surface and bulk structural consequences observed in a previous investigation [25] and summarized in Table 2.

References

[1] B. Imelik et al. (Eds.), Catalysis by Acids and Bases, Elsevier, Amsterdam, 1985.
[2] K. Tanabe, Solid Acids and Bases: Their Catalytic Properties, Academic Press, London, 1970.
[3] A.V. Deo, T.T. Chuang and I.G. Dalla-Lana, J. Phys. Chem., 75 (1971) 234.
[4] H. Knözinger, in B. Imelik et al. (Eds.), Catalysis by Acids and Bases, Elsevier, Amsterdam, 1985, pp. 111–125.
[5] G.A.M. Hussein, N. Sheppard, M.I. Zaki and R.B. Fahim, J. Chem. Soc. Faraday Trans. 1, 85 (1989) 1723.
[6] M.I. Zaki and N. Sheppard, J. Catal., 80 (1983) 114.
[7] T.H. Ballinger and J.T. Yates, Jr., Langmuir, 7 (1991) 3041.
[8] B. Delmon et al. (Eds.), Preparation of Catalysts, Vol. II, Elsevier, Amsterdam, 1979.
[9] R.-S. Zhou and R.L. Snyder, Acta Crystallogr. Sect. B, 47 (1991) 617.
[10] M.I. Zaki, G.A.M. Hussein and R.B. Fahim, Thermochim. Acta, 74 (1984) 167.
[11] N.S. Kurkova, Ya.R. Katsobashvili and N.A. Akchurina, Zh. Prikl. Khim. (Leningrad), 46 (1973) 1002.
[12] P.J. Gellings and H.J.M. Boumeester, Catal. Today, 12 (1992) 1.
[13] H.H. Kung, Transitional Metal Oxides: Surface Chemistry and Catalysis, Studies in Surface Science and Catalysis, Vol. 45, Elsevier, Amsterdam, 1989.
[14] Y.E. Nashed, M.Sc. Thesis, Minia University/Egypt, 1994.
[15] R.H. Pierson, A.N. Fletcher and E.St. Clair Gantz, Anal. Chem., 28 (1956) 1218.
[16] N.E. Fouad, H. Knözinger, M.I. Zaki and S.A.A. Mansour, Z. Phys. Chem., 171 (1991) 75.
[17] S. Soled, J. Catal., 18 (1983) 252.
[18] A.K.H. Nohman, M.I. Zaki, S.A.A. Mansour, R.B. Fahim and C. Kappenstein, Thermochim, Acta, 210 (1992) 103.
[19] G.T. Pott and B.D. McNicol, Discuss. Faraday Soc., 52 (1971) 121.
[20] L. Burlamacchi and P.L. Villa, React. Kinet. Catal Lett., 3 (1975) 199.
[21] D. Dollimore and J. Pearce, Surf. Technol., 10 (1980) 123.
[22] M.A. Baltanas, J.R. Katzer and A.B. Stiles, Acta Chim. Hung., 124 (1987) 341.
[23] R.G. Pearson, J. Am. Chem. Soc., 85 (1963) 3533; Chem. Eng. News, 43 (1965) 90; Chem. Br., 3 (1967) 103.
[24] A. Corma, G. Sastre, R. Viruela and C. Zicovich-Wilson, J. Catal., 136 (1992) 521.
[25] M.I. Zaki, A.K.H. Nohman, G.A.M. Hussein and Y.E. Nashed, J. Mater. Sci. Lett., 14 (1995) 1188.
[26] C. Kappenstein, T. Wahdan, D. Duprez, M.I. Zaki, D. Brands, E. Poels and A. Bliek, Proc. 6th Inter. Symp. Scientific Bases for the Preparation of Heterogeneous Catalysts, Elsevier, Amsterdam, 1985, pp. 699–706.
[27] P.G. Tsyrulnikov, V.A. Drozdov, V.S. Salnikov, S.A. Stuken, A.V. Kalinkin, Yu.A. Kachurovskii, P.Ye. Kolosov and Ye.I. Grigorov, Proc. 9th National Congress of Catalysis of India, 1980, POS-5.
[28] P.A.J.M. Angevaare, J.R.S. Aarden, J.R. Linn, A.P. Zuur and V. Ponec, J. Electron Spectrosc. Related Phenom., 54 (1990) 795.
[29] M.I. Zaki and H. Knözinger, Mater. Chem. Phys., 17 (1987) 201.
[30] M. Bensitel, V. Moravek, J. Lamotte, O. Saur and J.C. Lavalley, Spectrochim. Acta, 43A (1987) 1487.
[31] G. Busca and V. Lorenzelli, Mater. Chem., 7 (1982) 89.
[32] P. Fink, Rev. Roum. Chim., 14 (1969) 811.
[33] H. Knözinger, Adv. Catal., 25 (1976) 184.